PHYSICAL REVIEW B **77**, 201401(R) (2008)

Formation of silicon-fullerene-linked nanowires inside carbon nanotubes: A molecular-dynamics and first-principles study

Kengo Nishio,[1,*] Taisuke Ozaki,[2] Tetsuya Morishita,[1] and Masuhiro Mikami[1]

[1]*Research Institute for Computational Sciences (RICS), National Institute of Advanced Industrial Science and Technology (AIST), Central 2, Umezono 1-1-1, Tsukuba, Ibaraki 305-8568, Japan*

[2]*Research Center for Integrated Science (RCIS), Japan Advanced Institute of Science and Technology (JAIST), 1-1 Asahidai, Nomi, Ishikawa 923-1292 Japan*

(Received 13 March 2008; published 12 May 2008)

We study the formation of Si nanowires inside carbon nanotubes by using a combination of empirical molecular-dynamics and first-principles approaches. Molecular-dynamics simulations demonstrate that liquid Si encapsulated into a (13,0) nanotube crystallizes into a nanowire composed of linked Si_{16} fullerene cages. On the other hand, a nanowire composed of linked Si_{20} fullerene cages forms inside a (14,0) nanotube. The stabilities of these nanowires are further confirmed by first-principles calculations. We also find that the freestanding Si_{16}-linked nanowire is a metal, while the Si_{20}-linked nanowire is a semiconductor. The present findings suggest that the choice of the nanotube size allows us to control the structure of Si nanowires, and therefore to tailor the material properties.

DOI: 10.1103/PhysRevB.77.201401 PACS number(s): 61.48.−c, 62.23.Hj, 73.22.−f, 73.61.Wp

Si nanowires (Si NWs) have attracted much attention because of their potential uses in future nanoscale devices.[1–12] The electronic and optical properties of Si NWs are considerably different from those of bulk Si and dramatically depend on the wire diameter and atomic structure.[4,5,7] The stable atomic structure also depends on the wire diameter. Recent theoretical predictions indicate that Si NWs could have atomic structures not seen in the bulk Si.[3–5,9,10,12] These significant features lead to the idea of tailoring the properties of Si NWs for specific applications through the size and structure.

The use of nanoporous materials as templates is a powerful way of synthesizing nanomaterials in a controlled manner. The size and structure are determined by how the constituent atoms fit the interior space of nanopores. The usefulness of the template method has been demonstrated in various systems.[3,5,13–18] Even a single atomic chain, which is the ultimate nanowire, has been synthesized for gadolinium[18] and iodine[17] by using a carbon nanotube (CNT) as a template. Recent molecular-dynamics (MD) simulations have demonstrated that nonbulklike Si NWs, such as stacked-polygon nanotubes with diameters ranging from 0.34 to 0.48 nm (Ref. 5) and a polyicosahedral nanowire of 1.30 nm in diameter,[3] are formed by freezing liquid Si inside cylindrical nanopores. Here, the wire diameter is defined as the diameter of the smallest cylinder that contains the nanowire. In these MD studies, nanopores were assumed to be a chemically inert container for liquid Si and modeled by external potentials, which restrict the motion of Si atoms to cylindrical nanospaces. However, it is not clear whether such nanopores really exist.

We expect that CNTs can serve as such containers for the following reasons. First, silicon does not react with the surface of graphite.[6] Therefore, the wall of CNTs is expected to be inert to chemical reactions with silicon. Second, CNTs have high thermal stability. Actually, CNTs of 1.46 nm in diameter stood during heat treatment at 1873 K,[19] which is a considerably high temperature compared to the melting temperature of bulk Si (1685 K). Furthermore, the wall of CNTs was shown to be inert to chemical reactions with liquid Ge.[20] These all support the idea of exploiting CNTs as templates for Si NWs.

In this Rapid Communication, we demonstrate by using a combination of empirical MD and first-principles approaches the formation of Si NWs by freezing liquid Si inside CNTs. A nanowire composed of linked Si_{16} fullerene cages forms inside a (13,0) CNT of 1.03 nm in diameter. On the other hand, a nanowire composed of linked Si_{20} fullerene cages appears inside a (14,0) CNT of 1.11 nm in diameter. The Si_{16}- and Si_{20}-linked NWs with diameters of 0.53 and 0.61 nm, respectively, are larger than the stacked-polygon nanotubes and smaller than the polyicosahedral nanowire. The stabilities of Si-fullerene-linked NWs are further confirmed by the density functional theory (DFT) within the local density approximation (LDA).[21–24] We also find that the freestanding Si_{16}-linked NW is a metal, while the Si_{20}-linked NW is a semiconductor.

In our MD simulations, Si and C atoms were modeled by the Tersoff potential.[25] The Tersoff potential is known to provide an accurate description of covalent bonds in many forms of silicon, silicon carbide, and carbon,[25,26] which is necessary to simulate a multicomponent system comprised of a Si NW and a CNT. Our previous study of Si nanosheets inside slit pores showed that the Tersoff MD simulations and first-principles MD simulations yield essentially the same results,[27] suggesting that the result obtained by using the Tersoff potential is a good starting point for further sophisticated calculations.

Liquid Si consisting of 52 Si atoms was first prepared inside a (13,0) CNT consisting of 624 C atoms. Free boundary conditions were used for the system. The system was equilibrated at 2400 K ($1.02T_m$) by using Nosé–Poincaré thermostat.[28,29] Here, T_m (2350 K) is the melting point estimated for bulk Si by using the Tersoff potential. Although the CNT was partly distorted due to the thermal motion of C atoms, the overall structure stood at 2400 K. The system was then annealed at 1800 K ($0.77T_m$) for 15 ns. Figure 1(a) shows the time evolution of the interaction energy of Si

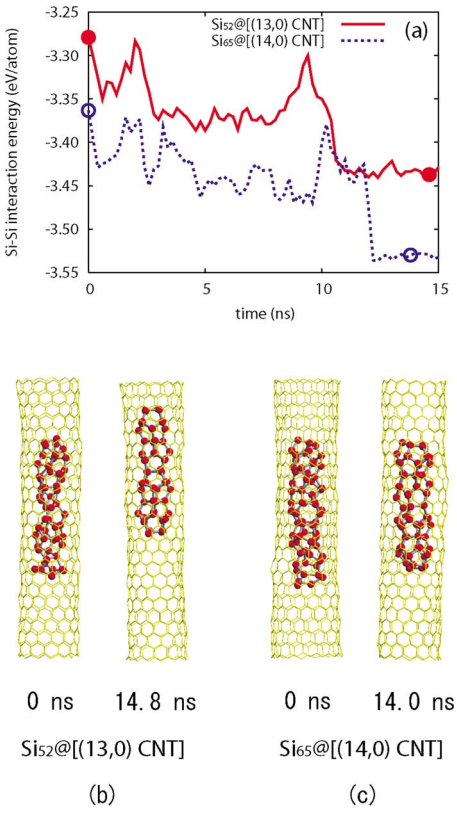

FIG. 1. (Color online) (a) Time evolution of the interaction energy of Si atoms for Si_{52}@[(13,0) CNT] (solid line) and Si_{65}@[(14,0) CNT] (dashed line). Snapshots of the atomic configurations corresponding to the filled and open circles are given in (b) and (c).

atoms averaged over 0.2 ns. The energy abruptly drops around 10 ns, which signifies the phase transformation of the encapsulated Si. Figure 1(b) demonstrates that the encapsulated liquid Si crystallizes into a nanowire constructed by linking four Si_{16} fullerene cages with D_{4v} symmetry. All the Si atoms in the nanowire are joined by tetrahedral bonding. The constituent Si_{16} cage has two square faces and eight pentagonal faces. The square faces face each other. Adjacent Si_{16} cages are linked together by sharing one square face. The fourfold symmetry axes of the Si_{16} cages coincide with the axis of the nanowire. We note that the Si_{16}-linked NW has no corresponding bulk structure in a sense that it cannot be made by cutting out any crystalline phases of bulk Si.

Similar MD simulations were performed for a system of 65 Si atoms encapsulated into a (14,0) CNT consisting of 672 C atoms [Figs. 1(a) and 1(c)]. In contrast to the system of Si_{52}@[(13,0) CNT], the Si_{16}-linked NW is not observed inside the (14,0) CNT. Instead, a nanowire constructed by linking four Si_{20} fullerene cages with D_{5v} symmetry appears. All the Si atoms in the nanowire are joined by tetrahedral bonding. The constituent Si_{20} cage has 12 pentagonal faces. Adjacent Si_{20} cages are linked together by sharing one pentagonal face. The fivefold symmetry axes of the Si_{20} cages coincide with the axis of the nanowire. We note that the Si_{20}-linked NW is a fragment of the framework of type-II Si clathrates.[6–8] In the bulk system, almost guest-free type-II Si clathrates are synthesized from guest-encapsulated ones by removing guest atoms.[30]

In order to clarify how the chirality of CNT and the number of Si atoms affect the structure of encapsulated Si NWs, we performed similar MD simulations for 120 Si atoms encapsulated into (10,4) and (12,4) CNTs. The diameters of (10,4) and (12,4) CNTs, which are 0.99 and 1.15 nm, are comparable to the diameters of (13,0) and (14,0) CNTs, respectively. The Si_{16}-linked NW formed inside the (10,4) CNT, while the Si_{20}-linked NW appeared inside the (12,4) CNT. These results indicate that the CNT diameter is the most important factor in determining the structure of encapsulated Si NWs.

The geometrical constraint alters the relative stability of Si-fullerene-linked NWs. The freestanding infinite Si_{20}-linked NW is energetically more stable by 0.102 eV/atom than the Si_{16}-linked NW. This is because the former contains pentagonal faces only, while the latter contains square and pentagonal faces.[1,31] The interior angle of a pentagon, which is 112°, is close to the ideal bond angle in tetrahedrally bonded structures, which is 109.47°. On the contrary, the angle of a square, which is 90°, deviates from the ideal angle. Therefore, the tetrahedrally bonded structure prefers pentagonal faces to square faces. The Si_{20}-linked NW fits the hollow space of the (14,0) CNT. However, the space of the (13,0) CNT is too narrow for the Si_{20}-linked NW. Therefore, the thinner Si_{16}-linked NW forms inside the (13,0) CNT.

We further examined the stabilities of Si-fullerene-linked NWs inside CNTs by using the DFT within the LDA. In our DFT calculations, norm-conserving pseudopotentials were used in a separable form with multiple projectors to replace the deep core potential into a shallow potential.[32,33] The wave functions were expressed by the linear combination of atomic orbitals centered on atomic sites. The atomic basis functions were generated by solving atomic Kohn–Sham equations by using confinement pseudopotentials.[34,35] The primitive pseudoatomic basis set, (Si6.5-$s2p2d1$), was used for Si, where the abbreviation Si6.5-$s2p2d1$ represents the employment of two primitive s orbitals, two primitive p orbitals, and one primitive d orbital of a Si atom, which were generated with a confinement radius of 6.5 bohr. The contracted pseudoatomic basis set, C4.5-$s31p31$, was used for C atoms, where $s31$ represents that one s orbital was generated by contracting three primitive s orbitals of a C atom. The contraction coefficients were optimized to minimize the total energy of a (13,0) CNT. The contracted bases improve the accuracy of the calculation without increasing the computational cost.[35] The real space grid techniques were used with the cutoff energy of about 120 Ry when calculating Hamiltonian matrix elements and solving the Poisson equation with a fast Fourier transformation.[36] All the DFT calculations were carried out by using the OpenMX code.[37]

To decrease the computational cost, we extracted systems of Si_{52}@C_{416} and Si_{65}@C_{448} from the systems obtained from the Tersoff MD simulations of Si_{52}@C_{624} and Si_{65}@C_{672}, respectively. These systems were then relaxed by an eigenvector following method[38] until the force on each atom becomes below 0.0003 and 0.0008 hartree/bohr for Si_{52}@C_{416} and Si_{65}@C_{448}, respectively. Figures 2(a) and 2(d) show the optimized structures of Si_{52}@[(13,0) CNT] and Si_{65}@[(14,0) CNT], respectively. No significant change is

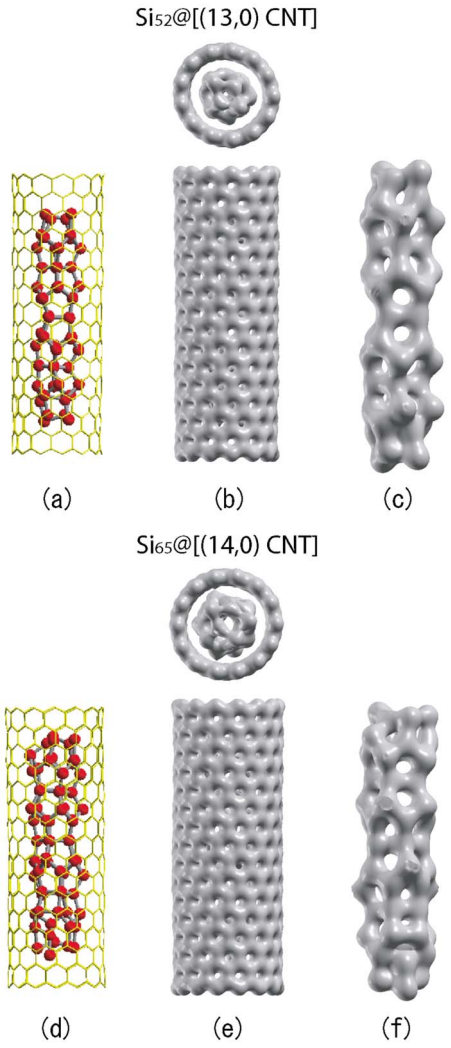

FIG. 2. (Color online) (a) Structure of Si_{52}@[(13,0) CNT] optimized by using the DFT calculations. (b) Isosurface (0.05 electrons/bohr^3) of the electron density for Si_{52}@[(13,0) CNT] (Ref. 42). (c) Isosurface (0.035 electrons/bohr^3) near the Si atoms. Results for Si_{65}@[(14,0) CNT] are given in (d)–(f).

observed in the overall Si-fullerene-linked structures except for local changes at the wire tips. The DFT calculations thus provide convincing evidence that Si-fullerene-linked NWs are stable inside CNTs.

The isosurface maps of electron density for Si_{52}@[(13,0) CNT] [Fig. 2(b)] and Si_{65}@[(14,0) CNT] [Fig. 2(e)] show that no covalent bond is formed between a Si NW and a CNT. This confirms the chemical inertness of CNT. We also find that C atoms are joined by sp^2 covalent bonding. Actually, electrons are localized along the lines joining each atoms. Figures 2(c) and 2(f) show that Si atoms apart from the wire tips are joined by sp^3 covalent bonding. The covalency in the bonds between the tip Si atoms is lowered. Actually, electrons are somewhat delocalized over the tip Si atoms. This delocalized nature of electrons is due to the rearrangement of Si atoms caused by coordination defects. The DFT calculations provide an accurate description of the tip structure, which the Tersoff potential fails because of the delocalized bonding.

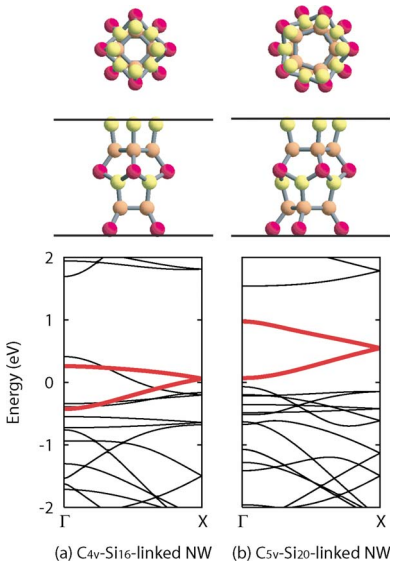

FIG. 3. (Color online) Electronic band structures of (a) C_{4v}-Si_{16}- and (b) C_{5v}-Si_{20}-linked NWs. Energy is measured from the Fermi energy. Bands drawn in bold (red) lines are the π bands of sp^2 bonded Si atoms. The unit cell of the nanowires is depicted in the upper parts. The vertical lines represent the optimized lengths of the unit cell, which are 1.048 nm (C_{4v}-Si_{16}-linked NW) and 1.068 nm (C_{5v}-Si_{20}-linked NW). The light gray (yellow) atoms are joined by sp^2-like bonds. The other atoms, which are the gray (orange) and dark gray (red) atoms, are joined by sp^3 bonds.

We further investigated the stabilities of Si-fullerene-linked NWs against the local cage distortion by using the DFT calculations. Calculations were performed for free-standing infinite nanowires because the [Si NW]@CNT composite systems are too large to tackle several possible configurations. The periodic boundary condition was applied along the wire axis. The unit cells of Si_{16}- and Si_{20}-linked NWs contain 24 and 30 Si atoms, respectively. Seven and five k-point samplings were used. Our DFT calculations revealed that the nanowires composed of lower-symmetry C_{4v}-Si_{16} and C_{5v}-Si_{20} cages are energetically more stable than the nanowires composed of D_{4v}-Si_{16} and D_{5v}-Si_{20} cages, respectively. The total energies of C_{4v}-Si_{16}-, D_{4v}-Si_{16}-, C_{5v}-Si_{20}-, and D_{5v}-Si_{20}-linked NWs are −3.9771, −3.9750, −3.9798, and −3.9754 hartree/atom, respectively. The higher stability of the lower-symmetry nanowires is attributed to the local atomic configurations, which resemble that of a stable Si(111)2×1 surface with buckled π-bonded chains.[39] All the Si atoms in the higher-symmetry nanowires are joined by three-dimensional sp^3 bonding, and 16 and 20 atoms per unit cell have one dangling bond in the D_{4v}-Si_{16}- and D_{5v}-Si_{20}-linked NWs, respectively. These threefold coordinated atoms are rearranged in the lower-symmetry nanowires [Figs. 3(a) and 3(b)] to form π-bonded chainlike structures, which resemble the reconstructed Si(111)2×1 surface. Actually, the light gray (yellow) atoms are joined by planer sp^2-like bonding and correspond to atom 11 in Ref. 39, and the outermost dark gray (red) atoms correspond to atom 12. The dangling bond energy is lowered by the formation of the π-bonded chainlike structure as in the case of the bulk surface. This explains why the lower-symmetry nanowires are

energetically more stable than the higher-symmetry nanowires. Note that when all the dangling bonds are terminated by hydrogen atoms, the reconstructed structure becomes unstable, and the hydrogen-terminated lower-symmetry nanowires transform to the higher-symmetry nanowires with ideal sp^3 bonds. The higher-symmetry structures might be stabilized by encapsulating guest atoms into fullerene cages as well.[40,41]

Figures 3(a) and 3(b) show the electronic band structures of lower-energy C_{4v}-Si_{16}- and C_{5v}-Si_{20}-linked NWs, respectively. Interestingly, the electronic structures are utterly different. The C_{4v}-Si_{16}-linked NW is a metal. On the other hand, the C_{5v}-Si_{20}-linked NW is a direct-band-gap semiconductor with a 0.14 eV band gap. This result is consistent with previous studies of the Si_{20}-linked NW.[7,8] The calculation of the radiative recombination rate revealed that the optical dipole transition between the lowest unoccupied and highest occupied molecular orbitals is prohibited, even though the C_{5v}-Si_{20}-linked NW is a direct-band-gap semiconductor. The position of the π band closely relates to the electronic properties. The π band of the metallic C_{4v}-Si_{16}-linked NW overlaps with other bands. On the other hand, in the semiconducting C_{5v}-Si_{20}-linked NW, the π band is separated from the other bands. We note that the hydrogen-terminated nanowires are semiconductor because dangling bond states are swept out from the fundamental gap region.

In summary, we have demonstrated that liquid Si encapsulated into a CNT crystallizes into a Si-fullerene-linked NW. The Si_{16}-linked NW forms inside a (13,0) CNT, while the Si_{20}-linked NW appears inside a (14,0) CNT. We have also shown that the freestanding Si_{16}-linked NW is a metal, while the Si_{20}-linked NW is a semiconductor. The present findings suggest that the physical properties of Si NWs can be tailored for specific applications through the structure which can be controlled by the choice of the CNT diameter.

K.N. wishes to thank T. Ikeshoji for fruitful discussions. This work is supported in part by METI (as part of the Nanoelectronics project) and the Next Generation Super Computing Project, Nanoscience Program. The computations were in part carried out at the Research Center for Computational Science, National Institute of Natural Sciences.

*k-nishio@aist.go.jp

[1] *Nanosilicon*, edited by V. Kumar (Elsevier, New York, 2007).
[2] B. K. Teo and H. Sun, Chem. Rev. (Washington, D.C.) **107**, 1454 (2007).
[3] K. Nishio, T. Morishita, W. Shinoda, and M. Mikami, J. Chem. Phys. **125**, 074712 (2006).
[4] K. Nishio, T. Ozaki, T. Morishita, W. Shinoda, and M. Mikami, Phys. Rev. B **77**, 075431 (2008).
[5] J. Bai, X. C. Zeng, H. Tanaka, and J. Y. Zeng, Proc. Natl. Acad. Sci. U.S.A. **101**, 2664 (2004).
[6] B. Marsen and K. Sattler, Phys. Rev. B **60**, 11593 (1999).
[7] M. Durandurdu, Phys. Status Solidi B **243**, R7 (2006).
[8] S. Sirichantaropass, V. M. García-Suárez, and C. J. Lambert, Phys. Rev. B **75**, 075328 (2007).
[9] Y. Zhao and B. I. Yakobson, Phys. Rev. Lett. **91**, 035501 (2003).
[10] M. Menon and E. Richter, Phys. Rev. Lett. **83**, 792 (1999).
[11] S. Yamada and H. Fujiki, Jpn. J. Appl. Phys., Part 2 **45**, L837 (2006).
[12] R. Kagimura, R. W. Nunes, and H. Chacham, Phys. Rev. Lett. **95**, 115502 (2005).
[13] K. Koga, G. T. Gao, H. Tanaka, and X. C. Zeng, Nature (London) **412**, 802 (2001).
[14] Y. Maniwa, H. Kataura, M. Abe, S. Suzuki, Y. Achiba, H. Kira, and K. Matsuda, J. Phys. Soc. Jpn. **71**, 2863 (1994).
[15] K. Nishio, W. Shinoda, T. Morishita, and M. Mikami, J. Chem. Phys. **122**, 124715 (2005).
[16] K. Nishio, J. Kōga, T. Yamaguchi, and F. Yonezawa, J. Phys. Soc. Jpn. **73**, 627 (2004).
[17] L. Guan, K. Suenaga, Z. Shi, Z. Gu, and S. Iijima, Nano Lett. **7**, 1532 (2007).
[18] R. Kitaura, N. Imazu, K. Kobayashi, and H. Shinohara, Nano Lett. **8**, 693 (2008).
[19] K. Méténier, S. Bonnamy, F. Béguin, C. Journet, P. Bernier, M. Lamy de La Chapelle, O. Chauvet, and S. Lefrant, Carbon **40**, 1765 (2002).
[20] Y. Wu and P. Yang, Adv. Mater. (Weinheim, Ger.) **7**, 520 (2001).
[21] P. Hohenberg and W. Kohn, Phys. Rev. **136**, B864 (1964).
[22] W. Kohn and L. J. Sham, Phys. Rev. **140**, A1133 (1965).
[23] D. M. Ceperley and B. J. Alder, Phys. Rev. Lett. **45**, 566 (1980).
[24] J. P. Perdew and A. Zunger, Phys. Rev. B **23**, 5048 (1981).
[25] J. Tersoff, Phys. Rev. B **39**, R5566 (1989).
[26] K. Moriguchi and A. Shintani, Jpn. J. Appl. Phys., Part 1 **37**, 414 (1998).
[27] T. Morishita, K. Nishio, and M. Mikami, Phys. Rev. B **77**, 081401(R) (2008).
[28] S. D. Bond, B. J. Leimkuhler, and B. B. Laird, J. Comput. Phys. **151**, 114 (1999).
[29] S. Nosé, J. Phys. Soc. Jpn. **70**, 75 (2001).
[30] J. Gryko, P. F. McMillan, R. F. Marzke, G. K. Ramachandran, D. Patton, S. K. Deb, and O. F. Sankey, Phys. Rev. B **62**, R7707 (2000).
[31] V. Kumar and Y. Kawazoe, Phys. Rev. B **75**, 155425 (2007).
[32] P. E. Blöchl, Phys. Rev. B **41**, 5414 (1990).
[33] N. Troullier and J. L. Martins, Phys. Rev. B **43**, 1993 (1991).
[34] T. Ozaki, Phys. Rev. B **67**, 155108 (2003).
[35] T. Ozaki and H. Kino, Phys. Rev. B **69**, 195113 (2004).
[36] J. M. Soler, E. Artacho, J. D. Gale, A. García, J. Junquera, P. Ordejón, and D. Sánchez-Portal, J. Phys.: Condens. Matter **14**, 2745 (2002).
[37] The code OpenMX, pseudoatomic basis functions, and pseudopotentials are available on a web site (http://www.openmx-square.org/).
[38] F. Eckert, P. Pulay, and H.-J. Werner, J. Comput. Chem. **18**, 1473 (1997).
[39] F. J. Himpsel, P. M. Marcus, R. Tromp, I. P. Batra, M. R. Cook, F. Jona, and H. Liu, Phys. Rev. B **30**, 2257 (1984).
[40] V. Kumar and Y. Kawazoe, Phys. Rev. Lett. **87**, 045503 (2001).
[41] A. K. Singh, V. Kumar, and Y. Kawazoe, Phys. Rev. B **71**, 115429 (2005).
[42] A. Kokalj, Comput. Mater. Sci. **28**, 155 (2003); code available from http://www.xcrysden.org/